

On the Coexistence of Macrocell Spatial Multiplexing and Cognitive Femtocells

Ansuman Adhikary
University of Southern California
Los Angeles, CA 90089, USA
adhikary@usc.edu

Giuseppe Caire
University of Southern California
Los Angeles, CA 90089, USA
caire@usc.edu

Abstract—We study a two-tier macrocell/femtocell system where the macrocell base station is equipped with multiple antennas and makes use of multiuser MIMO (spatial multiplexing), and the femtocells are “cognitive”. In particular, we assume that the femtocells are aware of the locations of scheduled macrocell users on every time-frequency slot, so that they can make decisions on their transmission opportunities accordingly. Femtocell base stations are also equipped with multiple antennas. We propose a scheme where the macrocell downlink (macro-DL) is aligned with the femtocells uplink (femto-UL) and, Vice Versa, the macrocell uplink (macro-UL) is aligned with the femtocells downlink femto-DL). Using a simple “interference temperature” power control in the macro-DL/femto-UL direction, and exploiting uplink/downlink duality and the Yates, Foschini and Miljanic distributed power control algorithm in the macro-UL/femto-DL direction, we can achieve an extremely attractive macro/femto throughput tradeoff region in both directions. We investigate the impact of multiuser MIMO spatial multiplexing in the macrocell under the proposed scheme, and find that large gains are achievable by letting the macrocell schedule groups of co-located users, such that the number of femtocells affected by the interference temperature power constraint is small.

I. INTRODUCTION

It is widely recognized that *spatial reuse* is the single most valuable resource to dramatically increase the throughput of wireless cellular networks. However, deploying a very dense cellular infrastructure, with base station (BS) density that grows *linearly* with the user density, is not viable for a number of obvious practical and economical reasons. On the other hand, user-deployed WLANs (e.g., IEEE 802.11) achieve such dense spatial reuse in the unlicensed band. This solution has the advantage of providing very high data rates for short-range, mostly in-home, communication, but does not handle mobility as efficiently as cellular systems. Therefore, *licensed* cellular systems are naturally evolving towards two-tier architectures, where a large number of user-deployed *femtocells* operate under a common macrocell “umbrella”, that fills in the gaps of the small cells tier and supports mobility. A large body of theoretical and standardization studies on this topic has been produced in recent years (for a small sample, see [1], [2], [3], [4], [5]).

Most existing works focus on continuous transmission of macrocell user terminals (macro-UTs) and on the calculation

of the pdf of the signal-to-interference plus noise (SINR) at given receivers, where the tail of the SINR pdf is related to the probability of outage. This approach disregards the fact that the forthcoming generation of cellular systems (notable, 3GPP LTE and IEEE 802.16m) is based on TDMA/OFDM, where dynamic scheduling is used in the macrocell tier for the downlink (macro-DL) and for the uplink (macro-UL). For a macro-BS equipped with M transmit antennas and serving up to M macro-UTs on any time-frequency slot, the set of served macro-UTs (and therefore their location in the cell) may change on a slot by slot basis. This gives a statistical multiplexing opportunity to the femtocell tier: in the macro-DL slots, only the femtocells in the vicinity of a served macro-UT create significant interference to the macrocell tier; in the macro-UL slots, only the femtocells in the vicinity of an active macro-UT suffer from significant interference from the macrocell tier.

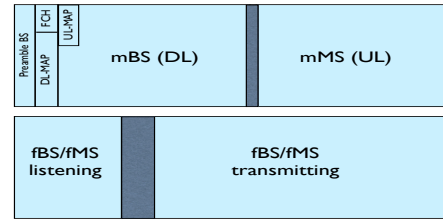


Fig. 1. Frame structure for the proposed cognitive femtocell system.

In order to exploit the implicit statistical multiplexing due to the macrocell dynamic scheduling, in [6] we proposed a “cognitive” approach to femtocells, where we assume that the femto-BSs and the femto-UTs can decode the macro-BS allocation map for both UL and DL. Fig. 1 shows a possible arrangement of macro and femto frames allowing cognitive operations, in the case where both tiers use time division duplexing (TDD). Assuming that the positions of all terminals are known,¹ the femtocells can regulate their transmit power in order to guarantee a given “interference temperature” to the macro-UTs. In Section II, we review the details of a scheme

¹Femtocells are deployed in fixed positions, that can be made available through a database. Macro-UTs are mobile, but their position changes sufficiently slow so that through GPS and radio localization their position can be provided at a slow rate as protocol side information by the macro-BS itself.

proposed in [6], based on linear beamforming and UL/DL duality, and we extend it to the case of multi-antenna macro-BS. Then, in Section III we discuss the coexistence of the multiuser MIMO (MU-MIMO) spatial multiplexing in the macrocell tier with the cognitive femtocells. In fact, it is intuitively clear that there is a tradeoff between the macrocell and the aggregate femtocell throughput: if the macrocell serves many macro-UT using spatial multiplexing, correspondingly many femtocells have to turn down their transmit power because of the interference temperature requirement, and therefore the femtocell throughput is decreased. In contrast, if the macro-BS serves only one macro-UT at each time-frequency slot, only a few femtocells are affected by the power control requirement but the macrocell tier does not exploit the full multiplexing gain and its throughput is decreased. We shall see that this problem is alleviated by scheduling approximately co-located groups of macro-UTs.

II. SIMO/MISO INTERFERENCE CHANNEL

We consider a single macro-BS with M antennas, serving $K \leq M$ macro-UTs. In the same coverage area, a set of femtocells share the same frequency band. Both tiers operate in TDD. The channel gains are formed by two components: a pathloss factor constant in time (over a large number of time-frequency slots) and frequency-flat, and a time-frequency selective small-scale fading that changes independently on a slot by slot basis. For simplicity, we focus here on a single subcarrier. By symmetry of the fading distribution, our results extend directly to an OFDM system with independent scheduling on each subcarrier.²

In the proposed scheme we have two types of slots: macro-DL/femto-UL and macro-UL/femto-DL (see Fig. 2). The femtocells operate in TDMA. Therefore, the number of femto-UTs actually present in each femtocell is irrelevant, since only one of them is active at any given slot and, for the sake of simplicity, it is sufficient to consider a single femto-UT per femtocell. Notice that the femtocells form a SIMO/MISO interference channel, coupled with the vector broadcast (DL) and multiaccess (UL) channel corresponding to the macrocell.

Macro-DL/Femto-UL slot: Macro- and femto-UTs are equipped with a single antenna. The received signal at the k -th macro-UT is given in general by

$$y_k = \sqrt{g(k, 0)} \mathbf{h}_{\text{mc},k}^H \sum_{i=1}^K \mathbf{v}_i x_{\text{mc},i} + \sum_{f \in \mathcal{C}} \sqrt{g(k, f)} h_{k,f} x_f + z_k \quad (1)$$

where $\mathbf{h}_{\text{mc},i} \in \mathbb{C}^{M \times 1}$ is the channel vector from the macro-BS antenna array to macro-UT i , \mathbf{v}_i is the corresponding macro-BS beamforming vector, \mathcal{C} denotes the set of all femtocells, $h_{k,f}$ is the scalar small-scale fading coefficient from femto-UT f to the macro-UT k , and $z_k \sim \mathcal{CN}(0, 1)$ is AWGN. The

²In general, a slight improvement can be obtained by scheduling jointly across the subcarriers. However, the improvement due to this more sophisticated multiuser scheduling across frequencies is marginal with respect to the system throughput achieved by the proposed scheme even with the suboptimal per-subcarrier scheduling.

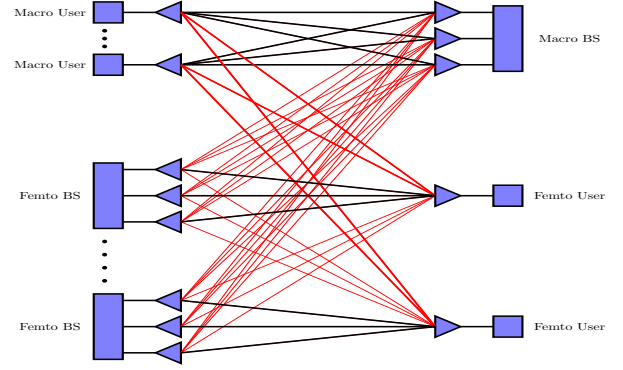


Fig. 2. Interference channel model for the two-tier network with multiple antennas at the femto-BSs and macro-BS. The thick red lines indicate the links that determine the femto user transmit power, via the interference temperature power control.

coefficients $g(a, b)$ indicate pathloss between points a and b , as detailed in Section III. The macro-BS is located at 0 (the origin of the cell coordinate system). The macro-BS calculates the beamforming vectors as functions of the matrix

$$\mathbf{H}_{\text{mc}} = [\mathbf{h}_{\text{mc},1}, \dots, \mathbf{h}_{\text{mc},K}], \quad (2)$$

formed by the K active macro-UTs, enumerated without loss of generality from 1 to K . This can be obtained either by TDD reciprocity (open-loop) or by explicit channel state feedback [7]. In particular, here we consider Linear Zero-Forcing Beamforming (LZFB), such that \mathbf{v}_i is given by the i -th column of the Moore-Penrose pseudo-inverse of \mathbf{H}_{mc} normalized to have unit norm. Hence, $\mathbf{h}_{\text{mc},k}^H \mathbf{v}_i = 0$ for all $i \neq k$. The macro-BS is subject to a total transmit power equal to P_0 , equally allocated over the K DL data symbols $x_{\text{mc},i}$.

The femto-UT in the f -th femtocell transmits with power $\mathbb{E}[|x_f|^2] = P_f$, regulated such that the interference caused at all active macro-UTs users is less than the target interference temperature κ . Hence, we have

$$P_f = \min \left\{ \frac{\kappa}{\max_{k \in \{1, \dots, K\}} g(k, f)}, P_1 \right\}, \quad (3)$$

where P_1 is the peak femtocell power. The SINR for macro-UT k is given by

$$\text{SINR}_k^{\text{mc-DL}} = \frac{g(k, 0) |\mathbf{h}_{\text{mc},k}^H \mathbf{v}_k|^2 \frac{P_0}{K}}{1 + \sum_{f \in \mathcal{C}} g(k, f) |h_{k,f}|^2 P_f} \quad (4)$$

and the corresponding instantaneous rate for macro-UT k on the current slot is given by $R_k = \log(1 + \text{SINR}_k^{\text{mc-DL}})$. For simplicity, we assume that the macro-BS schedules at each slot K out of $U \gg K$ macro-UTs, picked at random with equal probability. Hence, by averaging over the fading realization and the $\binom{U}{K}$ sets of macro-UTs, we obtain the sum-throughput of the macrocell tier in the DL. When $K = M$ and the fading is Rayleigh i.i.d., using the results in [8], this can be given in closed form for fixed U macro-UT positions.

The femto-BS receivers have L antennas each, and make use of linear MMSE detection, which maximizes SINR over all linear receivers. The received signal vector at a femto-BS f is given by

$$\mathbf{y}_f = \sum_{j \in \mathcal{C}} \sqrt{g(f, j)} \mathbf{h}_{f,j} x_j + \sqrt{g(f, 0)} \mathbf{H}_{f,0}^H \sum_{k=1}^K \mathbf{v}_k x_{\text{mc},k} + \mathbf{z}_f \quad (5)$$

The linear MMSE receive vector for estimating the desired symbol x_f from \mathbf{y}_f is given by $\mathbf{u}_f = \alpha_f \boldsymbol{\Sigma}_f^{-1} \mathbf{h}_{f,f}$ where $\alpha_f > 0$ is chosen such that $\|\mathbf{u}_f\| = 1$, and $\boldsymbol{\Sigma}_f$ is the interference-plus-noise covariance matrix in (5), given by

$$\begin{aligned} \boldsymbol{\Sigma}_f = \mathbf{I} + \sum_{j \in \mathcal{C}: j \neq f} g(f, j) \mathbf{h}_{f,j} \mathbf{h}_{f,j}^H P_j \\ + g(f, 0) \frac{P_0}{K} \mathbf{H}_{f,0}^H \left(\sum_{k=1}^K \mathbf{v}_k \mathbf{v}_k^H \right) \mathbf{H}_{f,0}. \end{aligned} \quad (6)$$

The receiver forms the scalar observation $\hat{y}_f = \mathbf{u}_f^H \mathbf{y}_f$, and the corresponding SINR is given by

$$\text{SINR}_f^{\text{fc-UL}} = P_f \mathbf{h}_{f,f}^H \boldsymbol{\Sigma}_f^{-1} \mathbf{h}_{f,f}. \quad (7)$$

Similarly to what argued before, the instantaneous rate of femtocell f is given by $R_f = \log(1 + \text{SINR}_f^{\text{fc-UL}})$. By summing over all the femtocells and averaging over the fading and the $\binom{U}{K}$ active macro-UTs sets (notice that they have an influence through the femtocell transmit powers P_f), we obtain the sum-throughput of the femtocell tier in the UL.

Macro-UL/Femto-DL: On the macro-UL/femto-DL slot, each femtocell has multiple antennas whereas the macro-UTs have single antenna each. Insisting on linear beamforming strategies, each femto-BS sends the L -dimensional signal vector $\mathbf{x}_f = \mathbf{w}_f s_f$, where \mathbf{w}_f denotes the transmit beamforming vector and s_f is the corresponding (coded) data symbol for its own intended femto-UT.

The received signal at the macro-BS is given by

$$\mathbf{y} = \sum_{k=1}^K \sqrt{g(k, 0)} \mathbf{h}_{\text{mc},k} x_{\text{mc},k} + \sum_{f \in \mathcal{C}} \sqrt{g(f, 0)} \mathbf{H}_{f,0} \mathbf{w}_f s_f + \mathbf{z} \quad (8)$$

The BS forms the scalar observation $\hat{y}_k = \mathbf{r}_k^H \mathbf{y}_k$ for detecting x_k , where \mathbf{r}_k is the receive beamforming vector for macro-UT k .

The received signal at the femto user in femtocell f is given by

$$y_f = \sum_{j \in \mathcal{C}} \sqrt{g(j, f)} \mathbf{h}_{f,j}^H \mathbf{w}_j s_j + \sum_{k=1}^K \sqrt{g(k, f)} h_{k,f}^* x_{\text{mc},k} + z_f. \quad (9)$$

Calculating the instantaneous SINRs $\text{SINR}_k^{\text{mc-UL}}$ and $\text{SINR}_f^{\text{fc-DL}}$ from (8) and from (9), respectively, is straightforward. In particular, from UL/DL duality (see [9]), extended to the MISO/SIMO interference channel in [10], we have that by letting $\mathbf{w}_f = \mathbf{u}_f$ and $\mathbf{r}_k = \mathbf{v}_k$, it is possible to achieve

$\text{SINR}_k^{\text{mc-UL}} = \text{SINR}_k^{\text{mc-DL}}$ and $\text{SINR}_f^{\text{fc-DL}} = \text{SINR}_f^{\text{fc-UL}}$ while preserving the total sum power, i.e., with

$$\sum_{f \in \mathcal{C}} Q_f + \sum_{k=1}^K Q_{\text{mc},k} = \sum_{f \in \mathcal{C}} P_f + P_0, \quad (10)$$

where $Q_{\text{mc},k}$ denotes the transmit power of macro-UT k and Q_f denotes the transmit power of the femto-BS f . The power allocation across the macro-UTs and the femto-BSs depends on the realization of the path losses and small scale fading components (which determine the beamforming vectors).

A. Implementation issues

In order to calculate the beamforming vectors \mathbf{u}_f , using the matrix inversion lemma we can write $\mathbf{u}_f = \beta_f \mathbf{K}_f^{-1} \mathbf{h}_{f,f}$, where $\beta_f > 0$ is another normalizing proportionality constant and \mathbf{K}_f is the received signal covariance matrix given by

$$\mathbf{K}_f = \boldsymbol{\Sigma}_f + g(f, f) \mathbf{h}_{f,f} \mathbf{h}_{f,f}^H P_f \quad (11)$$

Hence, the MMSE beamforming vectors can be conveniently calculated by using a sample covariance estimate of \mathbf{K}_f , from the whole received femto-UL slot, and an estimate of the desired signal channel $\mathbf{h}_{f,f}$ obtained by using UL pilots symbols, as in standard coherent detection for MIMO channels (e.g., currently implemented in IEEE 802.11n).

The other practical implementation problem of the proposed scheme consists of calculating the transmit powers $Q_{\text{mc},k}$ and Q_f in the macro-UL/femto-DL slot, for fixed unit-norm beamforming vectors $\mathbf{w}_f = \mathbf{u}_f$ and $\mathbf{r}_k = \mathbf{v}_k$. We propose to use the well-known Yates-Foschini-Miljanic distributed power allocation algorithm (see [11], [12]), that is guaranteed to converge to the solution.

For all femtocells f , fix the target DL SINR $\gamma_f^{\text{fc-DL}} = \text{SINR}_f^{\text{fc-UL}}$. For all active users k fix the target UL SINR $\gamma_k^{\text{mc-UL}} = \text{SINR}_k^{\text{mc-DL}}$. Let $\text{SINR}_f^{\text{fc-DL}}(\{Q_f\}, \{Q_{\text{mc},k}\}, \{\mathbf{u}_f\})$ denote the femtocell f DL SINR for fixed beamforming vectors and transmit powers, and let $\text{SINR}_k^{\text{mc-UL}}(\{Q_f\}, \{Q_{\text{mc},k}\}, \{\mathbf{u}_f\}, \{\mathbf{v}_k\})$ denote the macro-UT k UL SINR for fixed beamforming vectors and transmit powers. Then, the iterative distributed power control algorithm, in our case, is given by:

- 1) *Initialization:* let $n = 0$ and let $Q_{\text{mc},k}^{(0)} = P_0/K$, $Q_f^{(0)} = P_f$ for $k = 1, \dots, K$ and all $f \in \mathcal{C}$.
- 2) *Iterations:* for $n = 1, 2, 3, \dots$ do

$$\begin{aligned} Q_{\text{mc},k}^{(n)} &= \frac{Q_{\text{mc},k}^{(n-1)} \gamma_k^{\text{mc-UL}}}{\text{SINR}_k^{\text{mc-UL}}(\{Q_f^{(n-1)}\}, \{Q_{\text{mc},k}^{(n-1)}\}, \{\mathbf{u}_f\}, \{\mathbf{v}_k\})} \\ Q_f^{(n)} &= \frac{Q_f^{(n-1)} \gamma_f^{\text{fc-DL}}}{\text{SINR}_f^{\text{fc-DL}}(\{Q_f^{(n-1)}\}, \{Q_{\text{mc},k}^{(n-1)}\}, \{\mathbf{u}_f\})}. \end{aligned} \quad (12)$$

In order to implement this scheme, a sequence of adjacent slots should be allocated to the same group of K macro-UTs, and at each slot the receivers measure their SINR and report their measurements to the transmitters such that the power values can be updated according to (12).

TABLE I
SIMULATION PARAMETERS

| Parameter | Notation | Value |
|--------------------------------|---------------------|--------|
| Macro Cell Side Length | L | 1000 m |
| Path Loss Parameter | δ | 50 m |
| FC Radius | r_0 | 10 m |
| Distance between two FC | l | 40 m |
| Path Loss Exponent | α | 3.5 |
| Wall Partition Loss | w | 5 dB |
| Min SNR at cell edge | SNR_{\min} | 10 dB |
| Number of antennas at macro-BS | M | 8 |
| Number of antennas at femto-BS | L | 5 |

III. NUMERICAL RESULTS

In line with [6], we consider a unit-side square cell $[-1/2, 1/2] \times [-1/2, 1/2]$, with the macro-BS located at the origin 0, and F^2 femtocells are centered at points of coordinates $\left(\frac{2i-F+1}{2F}, \frac{2j-F+1}{2F}\right)$, for $i, j = 0, \dots, F-1$. Femtocells are disk-shaped with radius r_{fc} , shielded from the outdoor environment by walls. For two points a, b , the distance dependent path loss component is given by

$$g(a, b) = \frac{w^{n(a, b)}}{1 + (d(a, b)/\delta)^\alpha} \quad (13)$$

where $d(a, b)$ denotes the distance between a and b modulo the centered unit square (torus topology); $n(a, b)$ counts the number of walls between points a and b (i.e., $n(a, b) = 0$ if both a and b are outdoor or they are in the same femtocell, $n(a, b) = 1$ if either a or b is indoor (inside a femtocell), and $n(a, b) = 2$ if a and b are in different femtocells); w is the wall absorption factor; δ is the “3 dB” pathloss distance; α is the outdoor pathloss exponent.

We fix the macro-BS power P_0 such that the received SNR (without interference) for a macro-UT at the cell edge is 10 dB. By varying the value of the interference power temperature κ and letting $P_1 = 30$ dB,³ we obtain the Pareto boundary of the throughput tradeoff region achievable with the proposed scheme in the macro-DL/femto-UL slot, as described before. The tradeoff region for the dual channel, i.e., macro UL/femto DL is obtained by using the same beamforming vectors and the iterative power control algorithm. We distinguish between the cases of colocated and non-colocated macro-UTs. In the first case, we macro-BS schedules K users roughly located in the same position of the cell, such that they are separated enough to have independent small-scale fading, but they have the same pathloss with respect to the macro-BS and all the femtocells. In the second case, the K macro-UT positions are independently selected with uniform probability over the cell. Fig. 5 shows the comparison of the Pareto boundaries of the tradeoff regions for the colocated and non-colocated case (supremizing over K), showing a clear advantage for the colocated case, which is possible when the macro-UT density is large enough so that K approximately colocated users can be found. In all

³Assuming a peak rate in a femtocell in isolation is 10 bit/s/Hz, corresponding to uncoded 1024 QAM, we have $\text{SNR} = 10 \log_{10}(2^{10} - 1) = 10 * \log_{10}(1023) \approx 30$ dB.

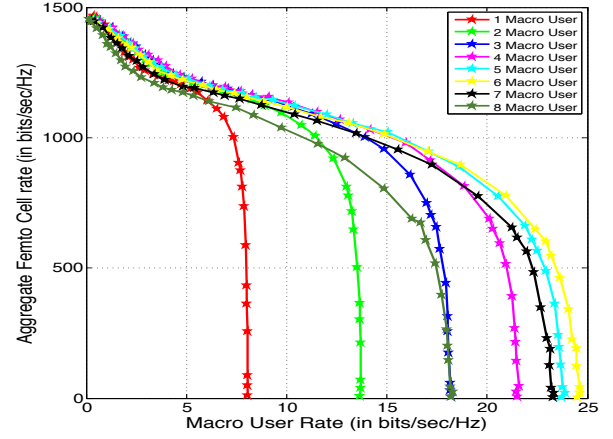


Fig. 3. Throughput tradeoff region comparison for colocated users in macro-DL/femto-UL. The different colors indicate the tradeoff region for different K .

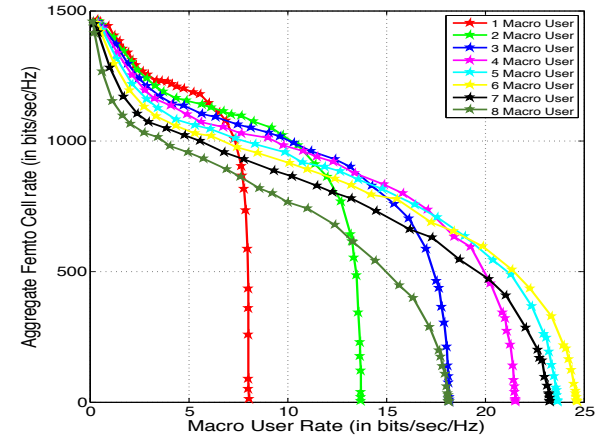


Fig. 4. Throughput tradeoff region comparison for non-colocated users in macro-DL/femto-UL. The different colors indicate the tradeoff region for different K .

the results, femtocells are assumed to be “open access”, therefore, macro-UTs are located only outdoor since a macro-UT inside a femtocell would be automatically “swallowed” by the femtocell, and served as a femtocell user. We already showed in [6] that the impact of closed-access femtocells is minimal, in contrast to what observed for conventional “legacy” systems, thanks to the proposed cognitive scheme and the interference temperature power control.

Figs. 3 and 4 show the throughput tradeoff region (femtocell sum throughput vs. macrocell sum throughput) achieved by the proposed scheme in the macro-DL/femto-UL slot (averaged over random user positions), for colocated and non-colocated macro-UTs, respectively. As the number of served macro-UTs increases, the macrocell throughput increases initially up to a certain maximum value (in our case, the highest macrocell throughput is obtained for $K = 6$ users) and then decreases. This can be expected from the typical behavior of linear LZFB precoding. For the non-colocated case, the

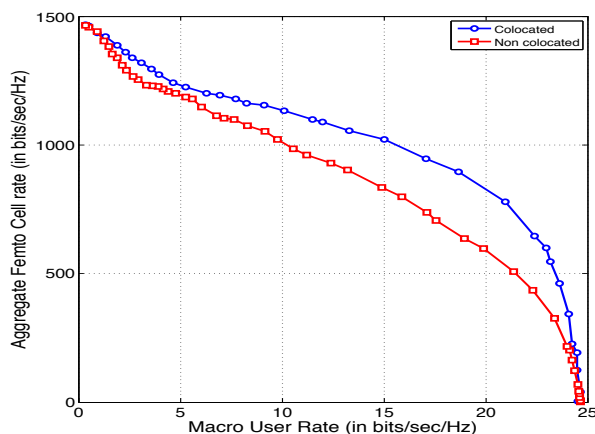


Fig. 5. Throughput tradeoff region comparison (Pareto boundary) between colocated and non colocated users in macro-DL/femto-UL.

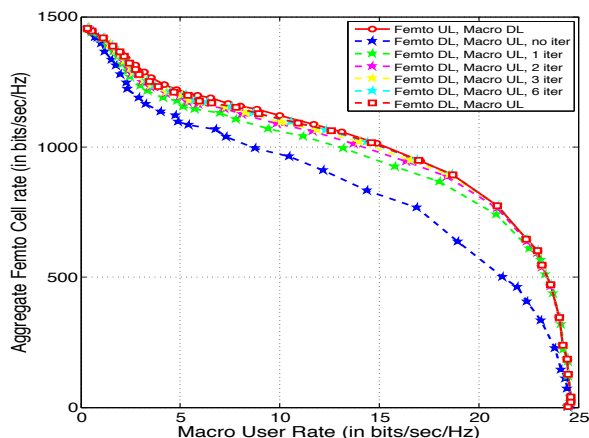


Fig. 6. Throughput tradeoff region for $K = 6$ colocated users in macro-UL/femto-DL for increasing iterations of the power control algorithm.

femto cell throughput decreases significantly as K increases, since more and more femto cells are affected by the power control interference temperature limitation. This is because K random macro-UTs positions are selected at each slot. Instead, for colocated macro-UTs, the value of K has no effect on the femto cell throughput, therefore, $K = 6$ achieves (approximately) uniformly best performance over the whole throughput range.

Fig. 6 and shows the throughput tradeoff region for the macro-UL/femto-DL slot, for $K = 6$ and different iterations of the power control algorithm. In every iteration of the power control algorithm, the peak power constraint is imposed for both the femto cells as well as the macro user terminals⁴. We notice that already for 3 iterations the algorithm yields almost the target “dual” macro-DL/femto-UL region, and for 6 iterations the region is indistinguishable. Notice also that because of the imposed peak power constraint, duality does

⁴In the macro-DL, each user is given an equal fraction of the power P_0 . In the macro-UL, each user is constrained to use a power no greater than P_0/K .

not strictly hold. Nevertheless, as seen from these plots, the impact of the peak power constraint on the macro-UL/femto-DL slot is basically negligible for this realistic range of system parameters.

IV. CONCLUSIONS

Overall, the ergodic rate region achievable by the proposed scheme is very competitive with other schemes proposed or analyzed in the current literature, considering that it can be achieved with a very simple protocol and low-complexity signal processing. For example, operating the system at the achievable throughput tradeoff point with macrocell throughput of 15 bit/s/Hz and femto cell throughput of 1000 bit/s/Hz, we can achieve 600 Mb/s over 40 MHz of system bandwidth of *average* macrocell symmetric data rate (both UL and DL), and 64 Mb/s per femto cell over the same system bandwidth (in our system geometry we have 625 femto cells per macro cell). Given these rather outstanding numbers, we believe that the proposed scheme is an attractive option for “beyond 4G” future wireless networks. Of course, several issues need further investigation, as for example the system operations and performance with multiple macro cells, the protocol overhead for implementing cognitive femto cells and adapting the power by the iterative algorithm, and the effect of scheduling co-located macro cell users on the macro cell user channel correlation, which may limit the effective macro cell multiplexing gain.

REFERENCES

- [1] S. Rangan, “Femto-Macro Cellular Interference Control with Sub-band Scheduling and Interference Cancellation,” *Arxiv preprint arXiv:1007.0507*, 2010.
- [2] V. Chandrasekhar, J. Andrews, and A. Gatherer, “Femto cell networks: a survey,” *IEEE Commun. Mag.*, vol. 46, no. 9, pp. 59–67, 2008.
- [3] S. Yeh, S. Talwar, S. Lee, and H. Kim, “WiMAX femto cells: a perspective on network architecture, capacity, and coverage,” *IEEE Commun. Mag.*, vol. 46, no. 10, pp. 58–65, 2008.
- [4] P. Xia, V. Chandrasekhar, and J. Andrews, “Open vs closed access femto cells in the uplink,” *Arxiv preprint arXiv:1002.2964*, 2010.
- [5] H. Dhillon, R. Ganti, F. Baccelli, and J. Andrews, “Modeling and analysis of k-tier downlink heterogeneous cellular networks,” *Arxiv preprint arXiv:1103.2177*, 2011.
- [6] A. Adhikary, V. Ntranos, and G. Caire, “Cognitive femto cells: Breaking the spatial reuse barrier of cellular systems,” in *Information Theory and Applications Workshop (ITA)*, 2011. IEEE, pp. 1–10.
- [7] G. Caire, N. Jindal, M. Kobayashi, and N. Ravindran, “Multiuser mimo achievable rates with downlink training and channel state feedback,” *Information Theory, IEEE Transactions on*, vol. 56, no. 6, pp. 2845–2866, 2010.
- [8] H. Kim, S. Lee, K. Lee, and I. Lee, “Transmission schemes based on sum rate analysis in distributed antenna systems,” *Arxiv preprint arXiv:1105.6199*, 2011.
- [9] P. Viswanath and D. Tse, “Sum capacity of the vector Gaussian broadcast channel and uplink-downlink duality,” *IEEE Trans. Inform. Theory*, vol. 49, no. 8, pp. 1912–1921, Aug. 2003.
- [10] F. Negro, I. Ghauri, and D. Slock, “Beamforming for the underlay cognitive MISO interference channel via UL-DL duality,” in *5th Int. Conf. on Cognitive Radio Oriented Wireless Networks and Communications (CROWNCOM)*. IEEE, pp. 1–5.
- [11] R. Yates, “A framework for uplink power control in cellular radio systems,” *Selected Areas in Communications, IEEE Journal on*, vol. 13, no. 7, pp. 1341–1347, 1995.
- [12] G. Foschini and Z. Miljanic, “A simple distributed autonomous power control algorithm and its convergence,” *IEEE Trans. Veh. Tech.*, vol. 42, no. 4, pp. 641–646, 1993.